Ratiometric Electrochemical Detection of Pd···π Interactions: Application Towards Electrochemical Molecular Logic Gates

Sean Goggins*[a], Oliver P. Stark[a], Christophe Naz[b], Barrie J. Marsh[b], and Christopher G. Frost[a]

*corresponding author

[a] Department of Chemistry, University of Bath, Claverton Down, Bath, BA2 7AY, UK. Email: s.goggins@bath.ac.uk

[b] Atlas Genetics Ltd, Derby Court, Epsom Square, White Horse Business Park, Trowbridge, Wiltshire, BA14 0XG, UK. Email: barrie.marsh@atlasgenetics.com

Abstract

The widespread and large scale use of platinum group metals, especially palladium, in a wide variety of industrial applications has seen their levels in wastewater streams, roadside dust and even pharmaceuticals significantly rise over recent years. Due to the possible environmental damage and potential health risk this may cause, there is now substantial demand for inexpensive, efficient and robust methods for the detection of palladium. Based upon self-immolative linker technologies, we have designed and synthesised a number of allyl ether-functionalised electrochemical probes to determine the optimum probe structure required to deliver a ratiometric electrochemical detection method capable of achieving a limit of detection of <1mg/mL within 20 minutes through the use of disposable screen-printed carbon electrodes. Combined with an enzymatic assay, this method was then used to achieve a proof-of-principle ratiometric electrochemical molecular logic gate.

1. Introduction

The extensive use of platinum group metals in the automotive, electronics and chemical industries, as well as having popular applications in jewellery and dentistry, has seen a sharp rise in the amount of these metals in waste streams (*1*). In particular, the concentration of platinum and palladium in a variety of environmental locations can be up to 70 times greater than that found in the earth's crust, which is attributed to metal loss from automotive catalytic converters through exhaust emissions (*2*–*5*). Despite rigorous purification techniques, metal contaminants found within medicinal compounds is also becoming commonplace and as this could pose a potential health risk (*6*), a low limit has been placed on the concentration of palladium impurities allowed to be found in drug substances (*7*). As a result, there is now a significant demand for efficient and sensitive protocols for palladium detection.

Highly sensitive palladium detection techniques include atomic absorption spectroscopy (AAS) (*8–9*), inductively-coupled plasma atomic emission spectrometry (10), mass spectrometry (*11–13*), X-ray fluorescence spectrometry (*14–15*), and solid-phase microextraction high performance liquid chromatography (SPME–HPLC) (*16*). Recently, substantial effort has been deployed for the development of a range of colourimetric and fluorescent probes for simple and effective palladium detection (*17*). To achieve greater sensitivity, palladium detection methodologies look to take advantage of the inherent catalytic attributes that the target possesses (*18*). For example, the catalytic Tsuji–Trost-like deallylation protocols pioneered by Koide and co-workers (*19–23*), allow rapid and sensitive palladium detection through the use of simple handheld UV lamps (*24*). Further sensitivity can also be achieved through small molecule autoinductive signal amplification systems if required (*25*). Electrochemistry is also becoming increasingly popular as an analyte detection method due to its low-cost, inherent miniaturisation capability and simple incorporation into point-of-care devices (*26–27*). Heavy metals such as cadmium, lead, mercury and arsenic can be detected using disposable, but modified, screen-printed electrodes but this is typically achieved through harsh stripping voltammetric methods (*28*). Herein, we describe the ratiometric electrochemical detection of palladium with unmodified screen-printed carbon electrodes using differential pulse voltammetry (DPV).

2. Results and Discussion

2.1 Ratiometric Electrochemical Detection of Palladium

Ratiometric electrochemical sensing can be achieved through either tagging both termini of nucleic acid capture probes bound to electrode surfaces with redox labels that have different oxidation potentials (*29–41*), manipulating host–guest or metal binding interactions on electrode surfaces with electrochemically distinguishable redox probes (*42–44*), or the use of redox-active probes which demonstrate a unique shift in oxidation potential selectively in the presence of the analyte (*45–46*). For analytes that display target catalysis as a means of amplification within diagnostic assays, we have found the latter offers a number of benefits, such as improved reaction kinetics, since probes are not surface bound, and ease of analysis, as electrodes do not require modification prior to detection (*47–48*). Continuing our goal of producing a suite of redox-active probes that enable the ratiometric electrochemical detection for a range of different analytes, we designed and synthesised a range of redox-active probes for the selective detection of palladium. To do this, we utilised ferrocene as the redox-active moiety due its well-understood Fe^{II}/Fe^{III} one-electron redox pathway and easy derivatisation (*49*), coupled covalently via a self-immolative linker (*50*), to an allyl trigger unit (Figure 1).

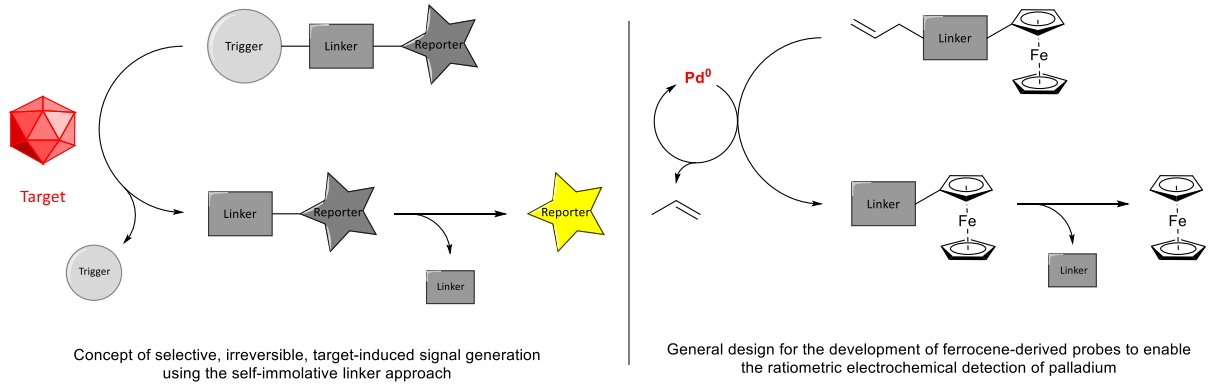

Fig 1. Concept of self-immolative linker-based sensing and its application towards the design of ratiometric electrochemical probes for selective palladium detection.

In the presence of the target therefore, oxidative insertion of the palladium into the allyl trigger would induce elimination of the linker and the subsequent entropically-favourable decarboxylation would release the ferrocene unit. Provided there is a noticeable change in electronic environment around the iron centre of the ferrocene, probe and product should be distinguishable electrochemically. It has been previously suggested that in order to achieve a ratiometric electrochemical detection method, probe and product should have a difference in oxidation potential (ΔE_{ox}) of approximately 100–200 mV (*51*). Thus, a number of probes that met the design criteria were synthesised (see ESI) and the oxidation potentials of both themselves and their respective elimination products were determined via DPV to ascertain the feasibility of the ratiometric detection method (Table 1).

Probe Structure	**Oxidation Potential (E_{ox1})**	**Product Structure**	**Oxidation Potential (E_{ox2})**	**Difference (ΔE_{ox})**
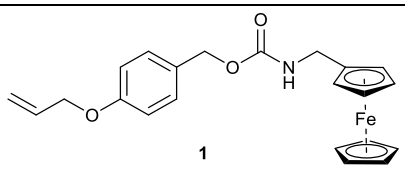 **1**	272 mV	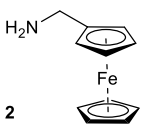 **2**	230 mV	42 mV
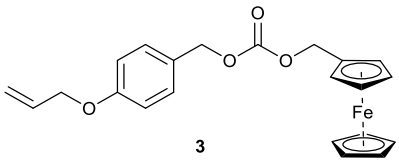 **3**	302 mV	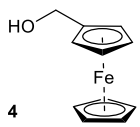 **4**	157 mV	145 mV

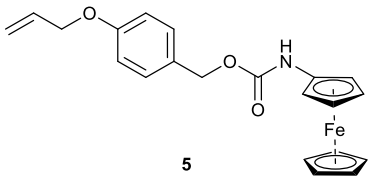 **5**	236 mV	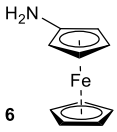 **6**	−141 mV	377 mV
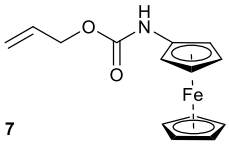 **7**	123 mV	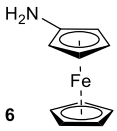 **6**	−141 mV	264 mV

Table 1 Structures and oxidation potentials of palladium-responsive ferrocene probes and their products. Oxidation potentials were determined using carbon graphite screen-printed electrodes at a ferrocene concentration of 0.77 mM in pH 8.9 Trizma® buffer referenced to Ag/AgCl.

Probe **1**, derived from ferrocenemethylamine **2**, was the first to be synthesised and tested, as benzyl carbamate linkers have shown good stability to unwanted hydrolysis within previous detection assays. However, the ΔE_{ox} between probe and product was found to be significantly lower than the ideal suggested ΔE_{ox} and possibly ruling out its use as a ratiometric electrochemical probe. This was confirmed through a duplex study where a solution containing both probe **1** and product **2** was analysed by DPV (see Fig. S1, ESI) and showed complete overlap of the peaks, thus preventing its use as a ratiometric electrochemical probe. Probe **3**, derived from ferrocenemethanol **4**, was next to be tried and tested as the change in heteroatom to a more electronegative atom should induce a greater difference in oxidation potential between probe and product; a worthwhile trade-off considering the use of the more unstable benzyl carbonate linker. As desired, the difference in oxidation potential was significantly increased and came within the ideal difference range. Unfortunately, a duplex study (see Fig. S2, ESI) still showed partial peak overlap which still prevents the use of the probe within a ratiometric detection method since accurate peak integrals cannot be obtained. In order to induce a greater difference in electronic environment around the ferrocene core between probe and product, we chose to remove the methylene unit between the ferrocene and the carbamate linkage. This alteration gave probe **5** and afforded a difference in oxidation potential between itself and aminoferrocene **6** of 377 mV; much greater than the difference needed to afford a ratiometric detection method. This was confirmed through another duplex study (see Fig. S3, ESI) where both peaks are clearly separated and the areas underneath them can be accurately integrated. However, initial test assays aimed to release aminoferrocene **6** in the presence of palladium were unsuccessful, which was presumed to be due to the slow elimination kinetics of the benzyl alcohol linker (*52*), and stability of the intermediate phenol under neutral pH. To alleviate this problem, probe **7** was simply synthesised without this linker. Probe **7** exhibited a lower oxidation potential to that of benzyl-linker containing probe **5** due to

its higher hydrophilicity; a known effect to cause significant changes in oxidation potential (*53*). However, the difference in oxidation potential was still >200 mV and as a duplex study displayed two clear distinct peaks (Figure 2), ratiometric detection was still feasible. As such, both peaks can be integrated accurately and conversion of probe to product can be calculated using the following equation:

$$\text{Conversion (\%)} = \left(\frac{\int \mathbf{6}}{(\int \mathbf{6} + \int \mathbf{7})}\right) \times 100$$

Pleasingly, when this probe was tested in the presence of palladium, aminoferrocene **6** was isolated in a 36% yield which can be attributed to palladium-catalysed deallylation of probe **7** followed by subsequent decarboxylation.

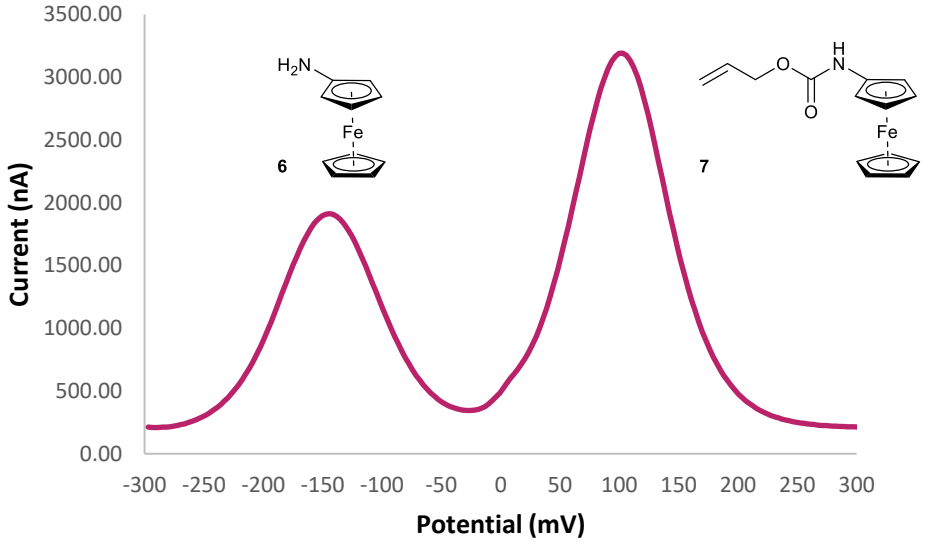

Fig. 2 Voltammogram of a solution containing 50 µM aminoferrocene **6** and 50 µM probe **7** in pH 8.9 Trizma® buffer.

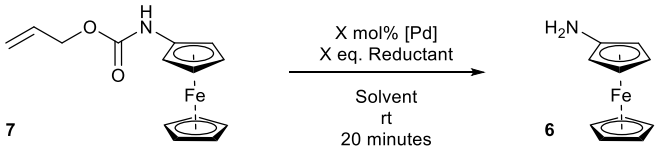

Entry	Pd Catalyst	Catalyst Loading	Reductant	Solvent	Conversion[a]
1	$Pd(PPh_3)_4$	10 mol%	Morpholine (10 eq.)	THF	100%
2	$Pd(PPh_3)_4$	5 mol%	Morpholine (10 eq.)	THF	6%
3	$Pd(PPh_3)_4$	5 mol%	$NaBH_4$ (10 eq.)	THF	91%
4	$Pd(PPh_3)_4$	1 mol%	$NaBH_4$ (10 eq.)	THF	93%
5	$Pd(PPh_3)_4$	0 mol%	$NaBH_4$ (10 eq.)	THF	6%
6	$Pd(PPh_3)_4$	1 mol%	$NaBH_4$ (10 eq.)	MeOH	100%
7	$Pd(PPh_3)_4$	1 mol%	$NaBH_4$ (1.1 eq.)	MeOH	100%
8	$Pd(PPh_3)_4$	0 mol%	$NaBH_4$ (10 eq.)	MeOH	0%
9	Pd_2dba_3	0.5 mol%	$NaBH_4$ (1.1 eq.)	MeOH	98%
10	$PdCl_2(PPh_3)_2$	1 mol%	$NaBH_4$ (1.1 eq.)	MeOH	67%

Table 2. Optimisation of conditions for the deallylation of probe **7** to aminoferrocene **6**. [a]Conversion determined by ratiometric electrochemical analysis

Having found an ideal probe for the ratiometric electrochemical detection of palladium, we first proceeded towards an optimisation (Table 2). Initially, classic palladium-catalysed conditions of $Pd(PPh_3)_4$ in THF were chosen with the inclusion of morpholine present as an allyl scavenger to regenerate the catalyst (Entry 1) (*54*). Pleasingly, in the presence of 10 mol% palladium, full conversion was observed within 10 minutes. However, halving the catalyst loading delivered less than 10% conversion. In order to improve the reactivity, and therefore the sensitivity, of the assay, the allyl scavenger morpholine was replaced with sodium borohydride, a commonly used hydride source in palladium-catalysed reductive deprotection of alloc groups (*55*). As desired, a dramatic increase in sensitivity was observed as 5 mol% $Pd(PPh_3)_4$ delivered near quantitative conversion after 20 minutes (Entry 3). Lowering the catalytic loading to 1 mol% furnished a similar conversion (Entry 4), demonstrating the sensitivity of the assay conditions. Importantly, in the absence of any palladium (Entry 5), a low background conversion was observed showing the stability of the carbamate linkage even in the presence of ten equivalents of a hydride. To further improve the reactivity of the assay, the solvent was changed from THF to methanol as this not only improves the solubility of the borohydride salt, but forms a more reactive methoxyborohydride species (*56*). As desired, this change led to an enhanced assay since full conversion was observed after just 5 minutes using only 1 mol% of catalyst (Entry 6). Reducing the equivalents of borohydride to 1.1 equivalents did not hinder reactivity as a similar

conversion rate was observed (Entry 7). No conversion was seen when the borohydride was removed completely demonstrating the stability of the alloc functional group even in the presence of metals, as well as highlighting the requirement of an allyl scavenging reagent to afford deallylation and subsequent conversion to product.

Other Pd^0 sources such as $Pd_2(dba)_3$ (Entry 9) and Pd^{II} sources such as $PdCl_2(PPh_3)_2$ (Entry 10) were found to give good conversion of probe **7** to product **6**, demonstrating the high selectivity of probe **7** for palladium whether in its 0 or +2 oxidation state. $Pd_2(dba)_3$ being a source of Pd^0 gave a similar quantitative conversion as observed with $Pd(PPh_3)_4$. To our surprise, the electrophilic Pd^{II} source, $PdCl_2(PPh_3)_2$ gave >60% conversion of probe **7** to aminoferrocene **6** as typically nucleophilic Pd^0 species are needed to achieve oxidative addition. Due to the presence of the reducing hydride source, it is presumed that Pd^{II} gets reduced to Pd^0 *in situ* before entering the catalytic deallylation cycle. Having studied the assay under different sources and oxidation states of palladium, we next looked at the effect of other metals (Figure 3).

Due to the well-known efficiency of palladium in such Tsuji–Trost-like reactions, the metal screen was conducted using 10 mol% catalyst to identify if any other metal could react with probe **7** in a similar fashion. Ni^{II} was shown to be the most active metal species delivering near quantitative conversion after 20 minutes. Similar to the Pd^{II} example previous, we presume that reduction of Ni^{II} to Ni^0 by $NaBH_4$ occurs *in situ* and this allows for the now nucleophilic metal species to catalyse the deallylation and decarboxylation of probe **7**. All oxidation states of rhodium and platinum tested were also found to be active within the assay giving >50% conversion over the 20-minute timeframe. This was expected since a whole range of different complexes are known to be active catalysts in Tsuji–Trost allylations (*57*). Of all the other metals screened including other platinum group metals such as iridium and ruthenium, none were able to give >30% conversion in the given assay time.

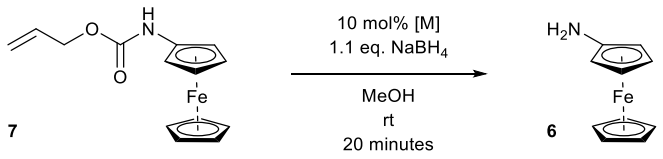

Fig. 3 Conversion of probe **7** to product **6** in the presence of different metals.

2.2 Application to an Electrochemical Molecular AND Logic Gate

Having investigated and explored the ratiometric electrochemical detection of palladium, we next wanted to apply the conditions to develop a proof-of-principle electrochemical molecular logic gate that utilises the ratiometric detection method as a signal output. Continuing from previous, we considered a concept where an AND molecular logic gate could be achieved if a reporter molecule could be linked via a self-immolative linker to two functional groups (FG) arranged in series (Figure 4). In order to initiate signal production and thus produce a positive output, both input A (to cleave the first functional group) and input B (to cleave the second functional group) must be present.

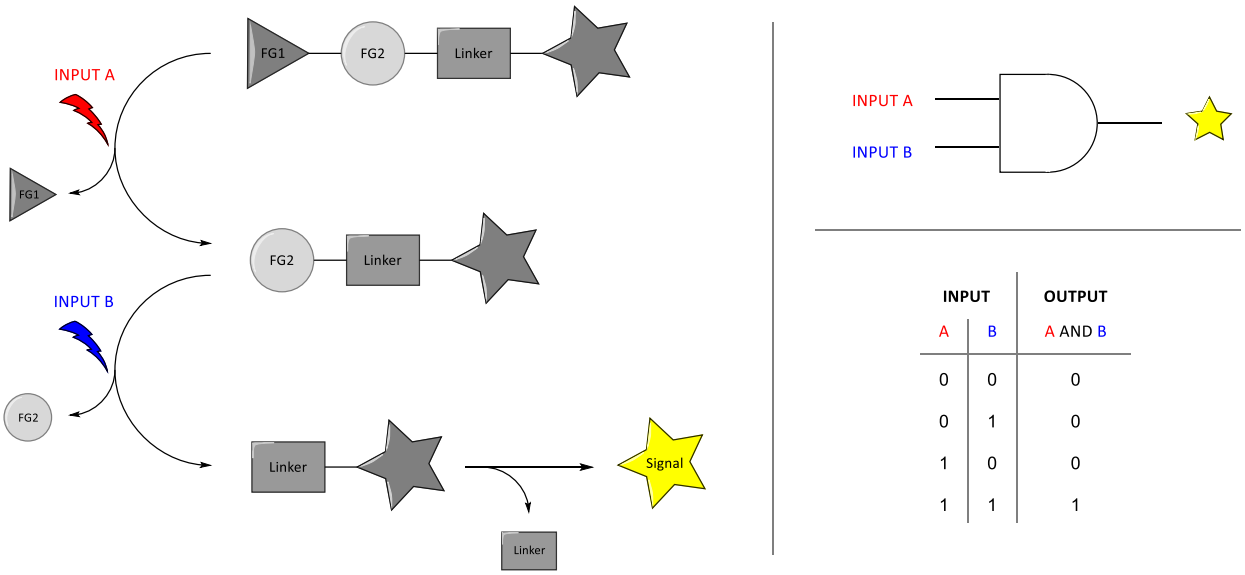

Fig 4. Design concept of a molecular AND logic gate based upon self-immolative linker-based sensing and the corresponding logic gate symbol and truth table.

To realise this potential, an aminoferrocene attached through a carbamate linkage to a benzyl linker with two sequential functional groups appended, one phosphate and one bis(allyl), was designed (Figure 5, probe **8**). In principle, this compound should act like a molecular AND logic gate as only in the presence of both palladium (input A = 1) and the enzyme alkaline phosphate (ALP, input B = 1) should both deallylation and dephosphorylation occur, which is needed to release aminoferrocene **6** (output = 1). If palladium is not present (input A = 0), the allyl functional groups attached to the phosphate should prevent dephosphorylation, as the phosphate dianion ($ROPO_3^{2-}$) is needed for the compound to be a suitable substrate for ALP, and therefore prevent signal production (output = 0). If ALP is not present (input B = 0), then deallylation can still occur (input A = 0) but dephosphorylation, needed to trigger immolation of

the linker and decarboxylation to release aminoferrocene **6**, is unable to occur (output = 0). In the absence of both palladium (input A = 0) and ALP (input B = 0), neither of the functional groups are able to be cleaved and no signal should be produced (output = 0).

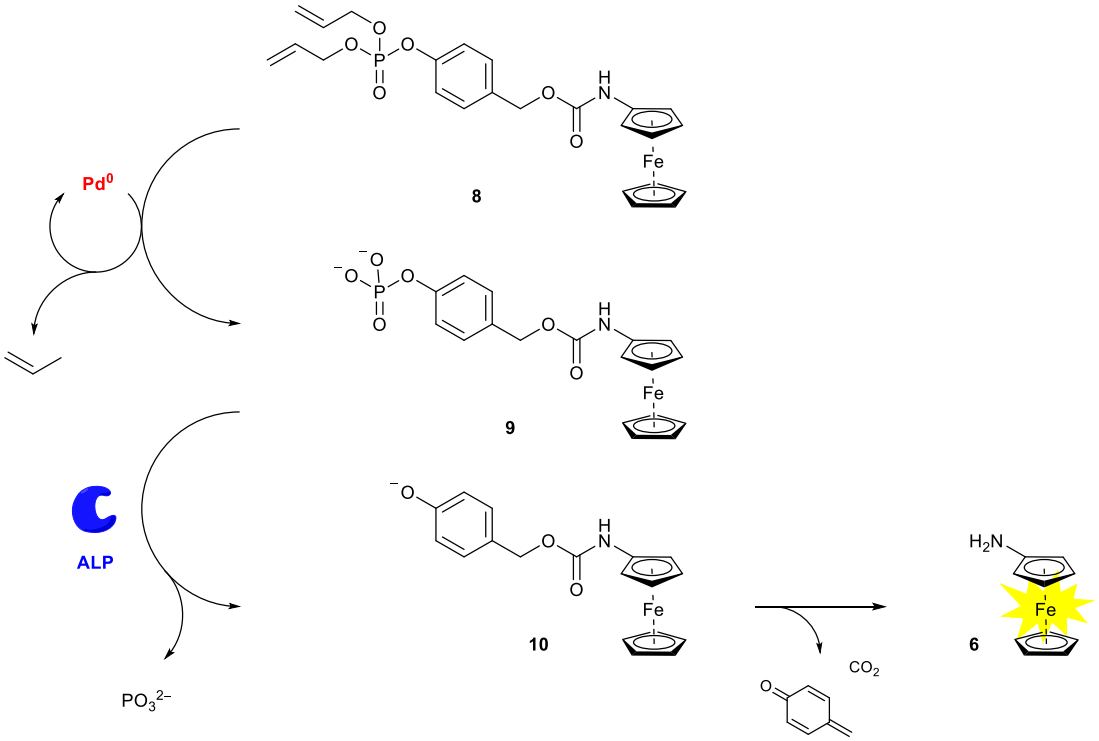

Fig 5. Structure for electrochemical molecular AND logic gate and proposed mechanism required to obtain positive signal production.

First, probe **8** was exposed to palladium under the reduction conditions as described above followed by treatment with an alkaline buffered solution of ALP before the mixture was analysed electrochemically. Unfortunately, under these reaction conditions, no aminoferrocene **6** was observed and the large number of components present in the assay solution led to indistinguishable peaks and a noisy voltammogram. With the one-pot process unsuccessful, we reverted back to our traditional conditions for deprotecting bis(allyl)phosphate protecting groups and initially monitored this transformation by thin layer chromatography (TLC) to determine the length of time required for full reaction conversion. Typically, 1 mol% of polymer-bound $Pd(PPh_3)_4$ requires 16 hours for complete deprotection of probe **8**. In order to accomplish the same feat in a more rapid time, we increased the catalytic loading to 100, 50 and 25 mol% and found that full consumption of probe **8**, as identified by TLC, occurred in approximately 45 minutes.

To verify this observation, the solution was then treated with a buffered solution containing 0.5 UmL^{-1} ALP and the assay monitored electrochemically (Fig. 6).

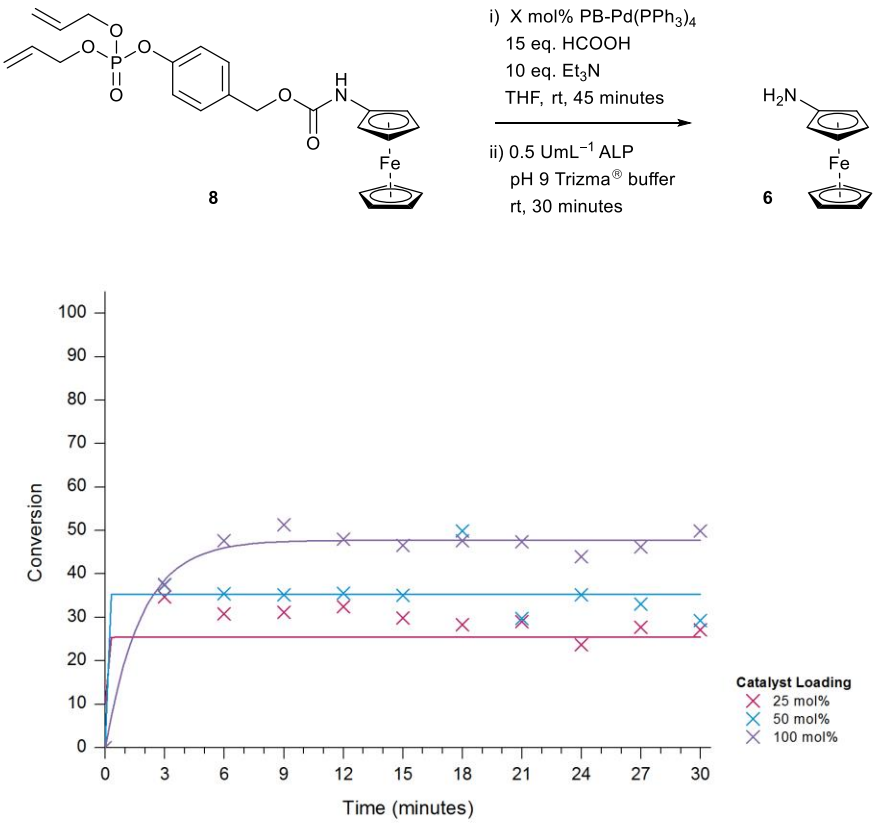

Fig. 6 Conversion of probe **8** to product **6** in the presence of different catalytic loadings of polymer-bound $Pd(PPh_3)_4$.

Pleasingly, under these conditions, positive conversion of probe **8** to aminoferrocene **6** was observed, demonstrating the applicability of the system to act like a molecular AND gate in the presence of both inputs. Minimal difference in conversion was seen under different catalytic loadings of the solid-supported palladium and as such, the highest loading was taken forward to maximise the level of conversion in the shortest length of time. The concentration of ALP was next to be investigated so the assay was repeated at 100 mol% polymer-bound $Pd(PPh_3)_4$ for 45 minutes followed by treatment with different concentrations of ALP (Fig. 7). Here, the optimal ALP concentration was found to be 12.5 UmL^{-1} as this delivered quantitative conversion after 30 minutes. With the optimised conditions in hand, we then went on to

determine the conversions, or the outputs, obtained under the conditions of different inputs to mimic a true logic gate (Table 3).

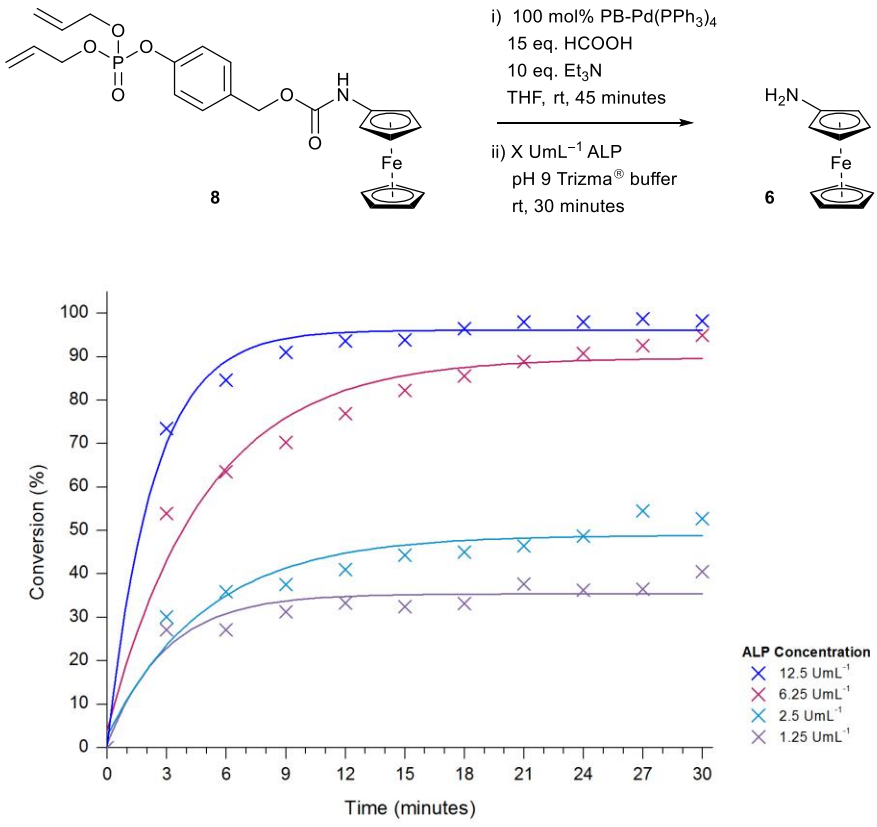

Fig. 7 Conversion of probe **8** to product **6** in the presence of different concentrations of ALP.

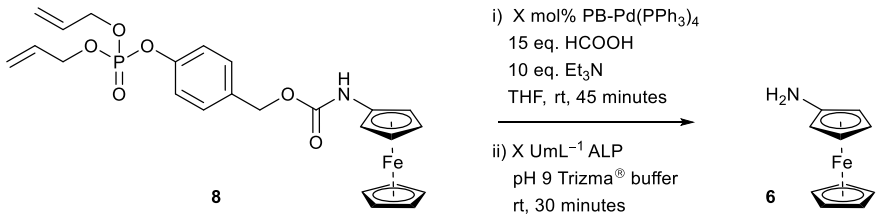

[Pd]	[ALP]	Conversion		INPUT A	INPUT B	OUTPUT
0 mol%	0 UmL^{-1}	0%		0	0	0
0 mol%	12.5 UmL^{-1}	0%		0	1	0
100 mol%	0 UmL^{-1}	0%		1	0	0
100 mol%	12.5 UmL^{-1}	100%		1	1	1

Table 3 Conversion of probe **8** to product **6** in the presence of none, either or both inputs.

As desired, only in the presence of both input values is any conversion observed. Interestingly, full conversion to aminoferrocene **6** is achieved, demonstrating significant confidence in the system that a definitive positive signal will only be returned in the presence of both input values (see Fig. S4, ESI for voltammogramatic overlays). Importantly, no background conversions were seen when either or both input values are null showing the excellent selectivity of the probe to the specific input signals.

3. Conclusion

In conclusion, we have developed a ferrocene-derived electrochemical probe for the ratiometric electrochemical detection of palladium. After a short optimisation, the detection was shown to be reasonably sensitive for palladium (0.77 mg/mL) using disposable screen-printed carbon electrodes in just 20 minutes. Selectivity was an issue however, as other metals such as nickel could also induce the production of a positive signal. To achieve a fully selective ratiometric electrochemical probe for palladium, further modifications of the probe will be investigated in due course. Additionally, the catalytic deallylation procedure was used to inspire development of a ferrocene-derived compound that could behave as a molecular electrochemical AND logic gate. Excellent control was demonstrated in this system as only when both inputs were present was any conversion, and therefore a positive signal, observed. We hope this work inspires the next generation of ratiometric electrochemical probes for more accurate and more reliable point-of-need sensing applications towards the detection of other analytes and the development of further electrochemical-based molecular logic gates.

4. Experimental

Electrochemical Analysis

Electrochemical analysis was performed by applying a 20 µL sample to screen-printed electrochemical cell (GM Nameplate, Seattle) equipped with a carbon graphite working electrode (2.36 mm^2), a carbon graphite counter electrode (10.15 mm^2) and a silver (pseudo Ag/AgCl) reference electrode (0.85 mm^2). The potential across the cell was controlled by a Metrohm Autolab PGSTAT30 potentiostat operated via a laptop running General Purpose Electrochemical System (GPES) software in differential pulse mode (modulation = 0.04 s, interval = 0.1 s, initial voltage = −500 mV, end voltage = 500 mV, step potential = 3 mV, modulation amplitude 49.95 mV). Peak integrals were obtained using the 'peak search' function and conversions calculated using the equation: $Conversion\ (\%) = \left(\frac{\int \mathbf{6}}{(\int \mathbf{6} + \int \boldsymbol{probe})}\right) \times 100$.

Synthetic procedure for probe 7

A stirring solution of ferrocenoyl azide (539 mg, 2.11 mmol, 1 eq.) in anhydrous toluene (7.2 mL) under argon was heated to reflux for 2 hours. After the temperature of the reaction was reduced to 90 °C, allyl alcohol (0.3 mL, 4.22 mmol, 2 eq.) was added and the reaction stirred for another 2 hours. Upon allowing the reaction to cool to room temperature, the mixture was concentrated under reduced pressure to afford the crude product. Purification by silica gel column chromatography (5% EtOAc in hexane) gave probe **7** as an orange solid (491 mg, 82%). **M.P.**; 81–83 °C. **IR**; ν 3271 (N–H), 3087 (C–H), 2938 (C–H), 2884 (C–H), 1690 (C=O), 1566 (C=O, amide). **^{1}H NMR** (300 MHz, C_6D_6); δ_H 5.76 (1H, ddt, *J* = 17.2, 10.6, 5.6 Hz), 5.34 (1H, br s), 5.14 (1H, dd, *J* = 17.2, 1.6 Hz), 4.99 (1H, dd, *J* = 10.6, 1.6 Hz), 4.51 (2H, d, *J* = 5.6 Hz), 4.41 (2H, br s), 4.03 (5H, s), 3.75 (2H, t, *J* = 2.0 Hz). **^{13}C NMR** (75 MHz, C_6D_6); δ_C 153.7, 133.3, 117.5, 96.4, 69.5, 65.7, 64.5, 60.9.

Synthetic procedure for probe 8

To a stirring solution of ferrocenoyl azide (255 mg, 1 mmol, 1 eq.) in anhydrous toluene (3 mL) under argon was added diallyl (4-(hydroxymethyl)phenyl) phosphate (284 mg, 1 mmol, 1 eq.) and the reaction mixture was heated to reflux for 2 hours. After cooling to room temperature, the reaction was concentrated under reduced pressure to afford the crude product. Purification by silica gel column chromatography (50% EtOAc in hexane) gave probe **8** as a dark orange oil (377 mg, 74%). **IR** (film, cm^{-1}); ν 3094 (N–H), 2953 (C–H), 1726 (C=O), 1259 (P=O), 1017 (P–O), 951 (C=C–H). **^{1}H NMR** (300 MHz, C_6D_6); δ_H 7.26 (2H, app

d, J = 8.3 Hz), 7.12 (2H, app d, J = 8.3 Hz), 6.81 (1H, br s), 5.71–5.58 (2H, m), 5.14 (2H, dd, J = 17.1, 1.3 Hz), 4.99 (2H, s), 4.92 (2H, dd, J = 10.4, 1.3 Hz), 4.47–4.33 (4H, m), 4.10 (5H, s), 3.81 (2H, app s). **^{13}C NMR** (75.5 MHz, C_6D_6); δ_C 154.1, 150.9 (d, $^2J_{C-P}$ = 7 Hz), 134.3, 132.5 (d, $^3J_{C-P}$ = 7 Hz), 130.1, 120.5 (d, $^3J_{C-P}$ = 5 Hz), 118.4, 97.0, 69.5, 68.9 (d, $^2J_{C-P}$ = 6 Hz), 65.9, 64.5, 60.9. **^{31}P {^{1}H} NMR** (121.5 MHz, C_6D_6); δ_P −4.70. **HRMS** (ESI): calc'd for $C_{24}H_{26}NaFeNO_6P$ $[M+Na]^+$ *m/z* 534.0745, found 534.0760.

Procedure for the ratiometric electrochemical detection of palladium

A 77 mM solution of probe **7** (5 mg, 0.01 mmol) dissolved in MeOH (1.3 mL) in a 2 mL screw-top sample vial, was subjected to the addition of sodium borohydride (4 mg, 0.11 mmol) followed by $Pd(PPh_3)_4$ (1 mg, 1 μmol). The assay was then stirred at 1000 rpm using a magnetic flea at room temperature and every 5 minutes thereafter, a 1 μL sample was taken from the assay, diluted by 1000 and thoroughly shaken. This diluted sample was then analysed electrochemically by the aforementioned method.

Procedure for molecular electrochemical logic gate tests

A 10 mM solution of probe **8** (5 mg, 0.01 mmol) dissolved in THF (1 mL) in a 2 mL screw-top sample vial, was subjected to the addition of polymer-bound $Pd(PPh_3)_4$ (13 mg, 0.01 mmol) followed immediately by formic acid (6 μL, 0.15 mmol) then triethylamine (14 μL, 0.10 mmol). The assay stirred at 1000 rpm using a magnetic flea at room temperature for 45 minutes. This solution was then added to a stirring solution of ALP (12.5 UmL^{-1}) in 50 mM pH 8.9 Trizma® buffer (9 mL). Every 3 minutes thereafter, a sample was analysed electrochemically by the aforementioned method.

Acknowledgements

The authors would like to acknowledge Atlas Genetics Ltd for their kind donation of a potentiostat and for the use of screen-printed electrodes.

Disclosure Statement

The authors declare no potential conflict of interest.

Supplementary Material

Material supplementary to this manuscript containing synthetic procedures and characterisation data can be found online at http://www.tandfonline.com/toc/gsch20/current

References

1. International Programme on Chemical Safety: *Palladium*, Environmental Health Criteria Series 226, World Health Organisation (WHO), Geneva, 2002.
2. Lee, D. S. *Nature*, **1983**, *305*, 47–48.
3. Hodge, V. F.; Stallard, M. O. *Environ. Sci. Technol.*, **1986**, *20*, 1058–1060.
4. Ely, J. C.; Neal, C. R.; Kulpa, C. F.; Schneegurt, M. A.; Seidler, J. A.; Jain, J. C. *Environ. Sci. Technol.*, **2001**, *35*, 3816–3822.
5. Boch, K.; Schuster, M.; Risse, G.; Schwarzer, M. *Anal. Chim. Acta.*, **2002**, *459*, 257–265.
6. Ravindra, K.; Bencs, L.; van Grieken, R. *Sci. Tot. Environ.*, **2004**, *318*, 1–43.
7. Garrett, C. E.; Prasad, K. *Adv. Synth. Catal.*, **2004**, *346*, 889–900.
8. Bergeron, M.; Beaumier, M.; Hébert, A. *Analyst*, **1991**, *116*, 1019–1024.
9. Kokya, T. A.; Farhadi, K. *J. Hazard. Mater.*, **2009**, *169*, 726–733.
10. Brown, R. J.; Biggs, W. R. *Anal. Chem.*, **1984**, *56*, 646–649.
11. Date, A. R.; Davies, A. E.; Cheung Y. Y. *Analyst*, **1987**, *112*, 1217–1222.
12. Castillo, M. L. A.; de Torres, A. G.; Alonso, E. V.; Cordero, M. T. S.; Pavón, J. M. C. *Talanta*, **2012**, *99*, 853–858.
13. Dimov, S. S.; Chryssoulis, S. L.; Lipson, R. H. *Anal. Chem.*, **2003**, *75*, 6723–6727.
14. van Meel, K.; Smekens, A.; Behets, M.; Kazandijian, P.; van Grieken, R. *Anal. Chem.*, **2007**, *79*, 6383–6389.
15. Ayres, Z. J.; Newton, M. E.; Macpherson, J. V. *Analyst*, **2016**, *141*, 3349–3357.
16. Kaur, V.; Aulakh, J. S.; Malik, A. K. *Anal. Chim. Acta.*, **2007**, *603*, 44–50.
17. Li, H.; Fan, J.; Peng, X. *Chem. Soc. Rev.*, **2013**, *42*, 7943–7962.
18. Goggins, S.; Frost, C. G. *Analyst*, **2016**, *141*, 3157–3218.
19. Song, F.; Garner, A. L.; Koide, K. *J. Am. Chem. Soc.*, **2007**, *129*, 12354–12355.
20. Garner, A. L.; Koide, K. *J. Am. Chem. Soc.*, **2008**, *130*, 16472–16473.
21. Garner, A. L.; Koide, K. *Chem. Commun.*, **2009**, 86–88.
22. Garner, A. L.; Song, F.; Koide, K. *J. Am. Chem. Soc.*, **2009**, *131*, 5163–5171.
23. Song, F.; Carder, E. J.; Kohler, C. C.; Koide, K. *Chem. – Eur. J.*, **2010**, *16*, 13500–13508.

24. Kitley, W. R.; Santa Maria, P. J.; Cloyd, R. A.; Wysocki, L. M. *Chem. Commun.*, **2015**, *51*, 8520–8523.
25. Baker, M. S.; Phillips, S. T. *J. Am. Chem. Soc.*, **2011**, *133*, 5170–5173.
26. Wang, J. *Biosens. Bioelectron.*, **2006**, *21*, 1887–1892.
27. Ronkainen, N. J.; Halsall, H. B.; Heineman, W. R. *Chem. Soc. Rev.*, **2010**, *39*, 1747–1763.
28. Hayat, A.; Marty, J. L. *Sensors*, **2014**, *14*, 10432–10453.
29. Du, Y.; Lim, B. J.; Li, B.; Jiang, Y. S.; Sessler, J. L.; Ellington, A. D. *Anal. Chem.*, **2014**, *86*, 8010–8016.
30. Gao, F.; Du, L.; Zhang, Y.; Tang, D.; Du, Y. *Anal. Chim. Acta*, **2015**, *883*, 67–73.
31. Xiong, E.; Zhang, X.; Liu, Y.; Zhou, J.; Yu, P.; Li, X.; Chen, J. *Anal. Chem.*, **2015**, *87*, 7291–7296.
32. Wang, T.; Zhou, L.; Bai, S.; Zhang, Z.; Li, J.; Jing, X.; Xie, G. *Biosens. Bioelectron.*, **2016**, *78*, 464–470;
33. Ren, K.; Wu, J.; Yan, F.; Ju, H. *Sci. Rep.*, **2014**, *4*, 4360.
34. Yu, P.; Zhou, J.; Wu, L.; Xiong, E.; Zhang, X.; Chen, J. *J. Electroanal. Chem.*, **2014**, *732*, 61–65.
35. Ren, K.; Wu, J.; Yan, F.; Zhang, Y.; Ju, H. *Biosens. Bioelectron.*, **2015**, *66*, 345–349.
36. Gao, F.; Qian, Y.; Zhang, L.; Dai, S.; Lan, Y.; Zhang, Y.; Du, L.; Tang, D. *Biosens. Bioelectron.*, **2015**, *71*, 158–163.
37. Xiong, E.; Wu, L.; Zhou, J.; Yu, P.; Zhang, X.; Chen, J. *Anal. Chim. Acta*, **2015**, *853*, 242–248.
38. Jia, J.; Chen, H. G.; Feng, J.; Lei, J. L.; Luo, H. Q.; Li, N. B. *Anal. Chim Acta.*, **2016**, *908*, 95–101.
39. Yeng, P.; Liu, Y.; Zhang, X.; Zhou, J.; Xiong, E.; Li, X.; Chen, J. *Biosens. Bioelectron.*, **2016**, *79*, 22–28.
40. Liu, Y.; Zhang, X.; Yang, J.; Xiong, E.; Zhang, X.; Chen, J. *Can. J. Chem.*, **2016**, *94*, 509–514.
41. Shen, W.-J.; Zhuo, Y.; Chai, Y.-Q.; Yuan, R. *Anal. Chem.*, **2015**, *87*, 11345–11352.
42. Yu, P.; Zhang, X.; Zhou, J.; Xiong, E.; Li, X.; Chen, J. *Sci. Rep.*, **2015**, *5*, 16015.
43. Chai, X.; Zhang, L.; Tian; Y. *Anal. Chem.*, **2014**, *86*, 10668–10673.
44. Zhang, X.; Wu, L.; Zhou, J.; Zhang, X.; Chen, J. *J. Electroanal. Chem.*, **2015**, *742*, 97–103.
45. Sagi, A.; Rishpon, J.; Shabat, D. *Anal. Chem.*, **2006**, *78*, 1459–1461.
46. Kesavan, M.; Mani, V.; Huang, S.-T. *RSC Adv.*, **2016**, *6*, 71727–71732.
47. Goggins, S.; Naz, C.; Marsh, B. J.; Frost, C. G. *Chem. Commun.*, **2015**, *51*, 561–564.
48. Goggins, S.; Marsh, B. J.; Lubben, A. T.; Frost, C. G. *Chem. Sci.*, **2015**, *6*, 4978–4985.
49. P. Štěpnička, *Ferrocenes: Ligands, Materials and Biomolecules*, John Wiley & Sons, Chichester, 2008.

50. Alouane, A.; Labruère, R.; Le Saux, T.; Schmidt, F.; Jullien, L. *Angew. Chem., Int. Ed.*, **2015**, *54*, 7492–7509.
51. McNeil, C. J.; Higgins, I. J.; Bannister, J. V. *Biosensors*, **1987/88**, *3*, 199–209.
52. Lee, H. Y.; Jiang, X.; Lee, D. *Org. Lett.*, **2009**, *11*, 2065–2068.
53. Marsh, B. J.; Hampton, L.; Goggins, S.; Frost, C. G. *New J. Chem.*, **2014**, *38*, 5260–5263.
54. Kunz, H.; Waldmann, H. *Angew. Chem., Int. Ed.*, **1984**, *23*, 71–72.
55. Beugelmans, R.; Neuville, L.; Bois-Choussy, M.; Chastanet, J.; Zhu, J. *Tetrahedron Lett.*, **1995**, *36*, 3129–3132.
56. Brown, H. C.; Ichikawa, K. *J. Am. Chem. Soc.*, **1961**, *83*, 4372–4374.
57. Minami, I.; Shimizu, I.; Tsuji, J. *J. Organomet. Chem.*, **1985**, *296*, 269–280.